JOURNAL OF CATALYSIS 116, 263–278 (1989)

Base Catalysis by Alkali-Modified Zeolites

I. Catalytic Activity

PAUL E. HATHAWAY AND MARK E. DAVIS[1]

Department of Chemical Engineering, Virginia Polytechnic Institute and State University, Blacksburg, Virginia 24061

Received June 12, 1988; revised September 27, 1988

Isopropanol is reacted over alkali-exchanged X and Y zeolites in the presence and absence of occluded exchange salts at 350°C and atmospheric pressure. The decomposition of cesium acetate occluded in CsNaY results in the generation of a very active base site. This site improves the acetone activity of the parent CsNaY by an order of magnitude. The CsNaX zeolite, however, does not contain this site after decomposition of the occluded cesium acetate and as a result shows an acetone activity comparable to that observed for the parent CsNaY. For the cesium acetate occluded CsNaY zeolite, the selectivity to acetone is above 97%, and on a surface area basis, the acetone activity is comparable to that found for MgO.

INTRODUCTION

The use of alkali-exchanged zeolites for base catalysis has received little attention, and even less attention has been directed toward the development and characterization of these sieves as solid bases. In characterizing these materials a technique for measuring both base strength and site distribution at reaction conditions would be ideal; however, no technique which combines these measurements is available (*1*).

Isopropanol decomposition has been employed to probe the acid and base properties of metal oxides at elevated temperatures (*2*). The assignment of the decomposition products to acid and base sites, however, deserves considerable caution. There is little question that over Brønsted acid sites, alcohols can dehydrate to form olefins by an elimination mechanism (*3*). The problem, however, is the possible misinterpretation that olefin activity is only a result of Brønsted acidity. It has been demonstrated that over metal oxides alcohols can dissociatively adsorb to form alkoxides (*4–6*). From the alkoxide intermediate, it has been suggested that dehydration or dehydrogenation can occur (*7–12*). Factors such as the structure (*2, 13*) and electronic nature (*8*) of the oxide surface as well as the structure (*7, 11, 12*) and partial pressure (*8*) of the reacting alcohol have been shown to influence the pathway of the reacting alkoxide. As a result, no clear distinction can be made between the olefins formed over Brønsted acid sites and those formed from the alkoxide decomposition. Furthermore, because of the many factors involved in the decomposition pathway of the alkoxide intermediate, it becomes increasingly difficult to know whether metal oxide catalysts which exhibit propylene activity will be effective in other base-catalyzed reactions.

There appears to be agreement with metal oxides that dehydrogenation occurs over basic sites (*4–12*). It, therefore, seems plausible for isopropanol decomposition that catalysts with high acetone activity and selectivity are likely to be effective in other base-catalyzed reactions as well. Thus, by developing molecular sieves which exhibit

[1] To whom correspondence should be addressed.

0021-9517/89 $3.00

high acetone activity and selectivity, we may expect that these sieves will be active in other base-catalyzed reactions.

An investigation on the basic nature of alkali-exchanged X and Y zeolites by isopropanol decomposition was reported by Yashima *et al.* (*14*). In that study, zeolite Y was shown to be more selective to acetone formation than zeolite X. The selectivity to acetone, however, never exceeded 50% at conversions above 22%. Nagy *et al.* (*15*) studied the decomposition of isopropanol to characterize the acid/base nature of K^{1+}- and Cs^{1+}-exchanged ZSM-5. At identical conversions, Cs–ZSM-5 was found to be more selective to acetone formation at 60%. However, Derewinski *et al.* (16) observed mainly propylene and higher oligomers in the decomposition of isopropanol over alkali-exchanged ZSM-5.

The base properties of alkali-exchanged X and Y zeolites have been investigated also by Barthomeuf (*17*) who examined pyrrole adsorbed on the zeolites by infrared spectroscopy. The results suggested the following order in base strength: CsX > RbX > KX > NaX > RbY > KY.

Alkali-exchanged X and Y zeolites have been investigated extensively for the base-catalyzed alkylation of toluene with methanol (*18–20*). From these studies, CsNaX is considered to be the most effective for side-chain alkylation over the other alkali-exchanged X and Y zeolites. The level of activity, however, appears to be the major obstacle in competing with present commercial processes.

Martens *et al.* (*21*) recently investigated large pore zeolites containing sodium clusters as base catalysts. From this study, it was suggested that framework oxygen anions in the neighborhood of intracrystalline neutral sodium clusters act as the active base site.

Base catalysis over alkali-exchanged molecular sieves is an area of growing interest. We have, therefore, systematically investigated the preparation and catalytic activity of alkali-exchanged X and Y zeolites in order to assess their ability to act as base catalysts.

EXPERIMENTAL

Materials. Zeolites X and Y were synthesized using the following gel compositions: 3.9 Na_2O:Al_2O_3 : 3.0 SiO_2 : 160 H_2O and 2.4 Na_2O : Al_2O_3 : 6.1 SiO_2 : 95 H_2O, respectively. For zeolite X, the gel was aged 4 h at 25°C and then heated for 13 hours at 100°C. In the case of zeolite Y, the gel was aged 48 hours at 25°C and then heated for 24 h at 100°C. The X zeolite crystallized without extraneous impurities, but the Y zeolite contained considerable amounts of amorphous material. The amorphous material was separated from the Y zeolite by stirring the mixture in deionized water, allowing the crystalline material to settle to the bottom, and discarding the supernatant liquid. Zeolites X and Y prepared by this procedure was found to be highly crystalline from both X-ray diffraction and nitrogen adsorption (*vide infra*). Isopropanol (99.5%) and all alkali salts were obtained from Aldrich. Helium (99.995%), oxygen (99.5%), and carbon dioxide (99.8%) were obtained from AIRCO, and used with no further purification.

Exchange procedure. Zeolites X and Y were exchanged at 25°C with 0.1 *N* solutions of group 1A metal hydroxides. All catalysts were exchanged at 0.02 g/ml. The exchange procedure involved three exchanges which were performed for 24-h time periods and a fourth exchange period which lasted 96 h. After each exchange, the catalysts were filtered and reslurried in fresh hydroxide solution. Upon completion of the 96-h exchange, the catalysts were filtered and left unrinsed to prevent decationation (*22*). The catalysts were then placed in a convection oven to dry at 100°C.

Cesium hydroxide, acetate, nitrate, and chloride were each used to exchange Cs^{1+} into zeolite Y. The exchange and drying process were identical to that described above except that after the final filtration,

half the filter cake was removed and left unrinsed, while the remaining half was rinsed with deionized water.

CsNaY was exchanged also in 0.3 and 0.5 *N* solutions of cesium acetate and left unrinsed in an attempt to occluded higher quantities of cesium acetate.

The amount of cesium exchanged into zeolite Y was varied using the following technique. Solutions varying in alkali composition, i.e., XCsOH : $(1 - X)$NaOH, where $0 \leq X \leq 1$ were prepared such that the total alkali was fixed at 0.1 *N*. The moles of CsOH in the solution were set by the desired loading of Cs^{1+} per unit cell. Again, the exchange was performed at 0.02 g/ml. Only one exchange was performed which lasted 192 h. From chemical analysis, it was determined that for lower loadings, e.g., ~8 Cs^{1+} per unit cell, nearly all the Cs^{1+} in the solution was exchanged. However, for higher loadings, some Cs^{1+} remained in the exchange solution.

Impregnation. Cesium acetate was impregnated into various supports using the following procedure. For a desired loading, a precalculated volume of a 0.025 *N* cesium acetate solution, e.g., 3 ml, was micropipetted into a vessel which contained the support. This mixture was then stirred overnight at ~40°C. The vessel was left open to air which allowed the water to slowly evaporate off. Using this procedure, a predicted 2.8 wt% loading for silica gel and activated carbon yielded (from chemical analysis) a ~2.4 wt% loading for both supports.

Analysis. Surface areas and pore volumes were determined by either nitrogen or oxygen adsorption on the Omnisorp I system developed by Omicron Technology.

Differential thermal analysis (DTA) was performed on a Dupont 900 differential thermal analyzer. Most samples were heated in air. One sample, however, was analyzed in a helium atmosphere. An empty sample pan was used as a reference.

Infrared measurements were performed on an IBM IR/32 FTIR spectrometer which was equipped with a high-temperature reaction cell similar to that reported by Hicks *et al.* (*23*). The window material was CaF_2 which is not infrared transparent below 1000 cm^{-1}.

Elemental analysis of the group 1A metal hydroxide-exchanged zeolites was performed by Galbraith Laboratories, Inc. (Knoxville, TN). All other elemental analyses were performed in our laboratories by inductively coupled plasma or atomic absorption spectrometry.

Because of the many variables considered in the exchange of zeolites X and Y, a nomenclature was adopted. For example, consider CsNaY–OH-UR. Here, cesium was exchanged into zeolite Y, the exchange was performed from the hydroxide (OH), and the filter cake was left unrinsed (UR) after the final exchange. When necessary, the degree of ion exchange will be given, e.g., $Cs_{39}Na_{18}Y$–OH-UR.

Reactor system and procedure. Isopropanol was pumped with a syringe pump into a 125°C constant temperature vaporizer where it was mixed with helium. This mixture could then bypass or feed into a vertical, down flow, fixed bed microreactor. The microreactor consisted of a 3 mm i.d. vycor tube placed inside a tube furnace. Two start-up procedures were used and will be described in the following sections.

The zeolite catalysts were compacted without binder into pellets which were subsequently crushed and size separated. The resulting particles were −60/+80 mesh. Because the chemical composition differs for each catalyst, the weight per unit volume changes. For example, the CsNaX prepared here weighs 34% more than the NaX per unit volume. Therefore, the differences in rates between CsNaX and NaX on a gram basis could be misleading because there are less zeolite unit cells or supercages in a gram of CsNaX than in a gram of NaX. However, the number of supercages in a mole of CsNaX unit cells is equivalent to that found in a mole of NaX unit cells. Therefore, reaction rates have been nor-

malized to a unit cell basis, i.e., moles of acetone or propylene formed per mole of zeolite unit cells per hour. Futhermore, because zeolites X and Y have identical crystal topologies, a direct comparison of activities between zeolites X and Y can be made on a unit cell basis.

The following conditions were found to give intrinsic reaction rate data: flow rates (STP) of helium and isopropanol were 180 and 45 ml min^{-1}, respectively, the reaction temperature was 350°C, and space velocities were above 6.7 mol isopropnaol · (mol of zeolite unit cells)$^{-1}$ · sec^{-1}. Reaction products were analyzed by an on-line gas chromatograph which employed a Porapak T column ($\frac{1}{8}$ in. × 12 ft) and a thermal conductivity detector. Response factors were measured and found to be in excellent agreement to those reported by Dietz (*24*).

RESULTS AND DISCUSSION

Physical properties. The composition, pore volume, and surface area of zeolites X and Y exchanged with the alkali hydroxides are given in Table 1. From bulk chemical analysis, the Si/Al ratio for zeolites X and Y is 1.34 and 2.34, respectively. The percentage exchange was determined also and is listed for each catalyst. Because these catalysts were left unrinsed after the final filtration, an excess of alkali was detected for several catalysts and is listed in Table 1. The percentage excess listed is defined as the number of excess M^{1+} per framework Al^{3+} times 100%. This calculation assumes all Na^{1+} atoms are balancing framework charge. From the Si/Al ratio, the percentage exchanged, and the percentage excess (assumed to exist as MOH), the molecular weight of the unit cell can be calculated and is listed in Table 1. Note that as Na^{1+} was exchanged by the heavier alkali metals the weight of the unit cell increases. Thus, all reaction rates reported in this work are normalized to a unit cell basis unless specified otherwise.

Because of the high electron density associated with the Rb^{1+} and Cs^{1+}-exchanged zeolites, X-ray powder diffraction was found to be ineffective for determining crystallinity. Therefore, the degree of crystallinity for each material was determined by measuring pore volumes and surface areas via nitrogen adsorption at 77 K. The pore volumes normalized to a gram basis for NaX and NaY are 0.34 and 0.35 ml/g, respectively. These values are in excellent agreement with 0.32 and 0.35 ml/g given by Breck (*25*) for NaX and NaY, respectively. The pore volumes listed in Table 1, however, are normalized to a supercage basis

TABLE 1

Physical Data of Zeolite Catalysts

Catalyst	Si/Al	% Exchanged[a]	% Excess	Molecular wt per unit cell	Volume (Å^3/supercage)[b]	BET area (m^2/g)[c]
NaX	1.34	—	—	13,330	927	875
KNaX	1.34	82	—	14,350	889	785
RbNaX	1.34	68	—	16,810	859	657
CsNaX	1.34	51	—	17,870	781	550
NaY	2.34	—	12	13,060	943	900
KNaY	2.34	93	23	14,380	910	795
RbNaY	2.34	71	15	16,230	810	623
CsNaY	2.34	63	—	16,770	694	526

[a] Based on a unit cell composition of: NaY, $Na_{58}Al_{58}Si_{134}O_{384}$; NaX, $Na_{82}Al_{82}Si_{110}O_{384}$.
[b] Calculated from nitrogen adsorption at 77 K and 300 Torr.
[c] BET surface areas calculated from nitrogen adsorption data.

(eight supercages per unit cell) as opposed to a weight basis in order to account for the differences in molecule weight. Thus, differences in the volume of nitrogen adsorbed by each catalyst are a result only of changes in available pore volume. Note that as Na^{1+} is exchanged by larger cations, the volume per supercage decreases accordingly.

Influence of start-up. Two start-up procedures were employed. Procedure 1, which was used for all reaction rate determinations, began by heating the catalyst in flowing helium (unless stated otherwise) to a specified calcination temperature, e.g., 550°C. After a 4-h calcination, the temperature was decreased to 450°C and the reactant flow initiated. The reaction was run for 30 min at 450°C. Next, the reaction temperature was lowered to 350°C and the system was allowed to reach steady state prior to rate measurements. Procedure 1 was found to ensure that the system maintained a steady-state conversion to both acetone and propylene (*vide infra*). Procedure 2, which was used to study the transient kinetic behavior of the system, involved the same calcination conditions as procedure 1, but the reaction temperature was lowered directly to 350°C before initiation of the reactant flow. The acetone activity obtained with procedure 1 was greater than that of procedure 2 by approximately 25% while the propylene activity showed little dependence on start-up. The cause of this difference in acetone activity is unknown to us at this time.

Intrinsic rates. Rates were determined at differential conversions. By varying the contact time, the rate of isopropanol decomposition was found to be independent of conversion for conversions below 3.5%. To test whether the measured rates were limited by diffusion, a plot of the ln (rate) versus $1/T\,K^{-1}$ was constructed for the acetone and propylene activity of CsNaY–OH-UR and is shown in Fig. 1. No curvature is observed for temperatures below 375°C for both acetone and propylene formation. Also, no curvature is observed when the gaseous flow rate was lowered (Fig. 1) thus excluding film diffusion limitations. From these data an activation energy can be determined for acetone and propylene formation over CsNaY–OH-UR. The activation energy for propylene formation is 24 kcal · mol^{-1} which is within the range reported by Jacobs *et al.* (*26*) for NaY. The activation energy of acetone formation is 37 kcal · mol^{-1}. A value of the activation energy for acetone formation over alkali-exchanged zeolites could not be found in the open literature; however, our value agrees well with the 37 kcal · mol^{-1} reported by Waugh *et al.* (*10*) for the formation of acetone over ZnO using a temperature-programmed reaction.

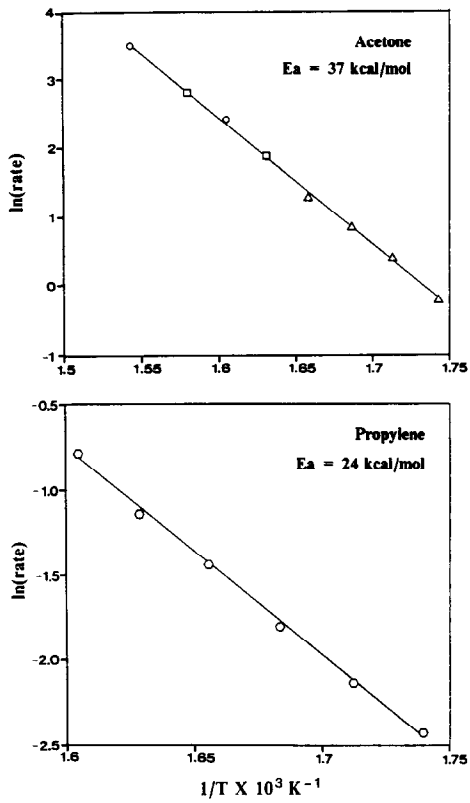

FIG. 1. Temperature dependence of activities. Acetone: ○, F/W = 3.6 mol isopropanol · h^{-1} · g^{-1}; □, F/W = 3.6 mol isopropanol · h^{-1} · g^{-1}; △, F/W = 0.90 mol isopropanol · h^{-1} · g^{-1}; propylene: ○, F/W = 0.90 mol isopropanol · h^{-1} · g^{-1}. Total pressure = 1 atm, and partial pressure of isopropanol = 152 Torr.

TABLE 2

Intrinsic Reaction Rate Data[a]

	Catalyst	Calcination atmosphere	Acetone rate[e]	Propylene rate[e]	% Acetone selectivity[f]
(A)	NaX^b	He	70	2003	3.4
	$KNaX^b$	He	295	88	77.0
	$RbNaX^b$	He	264	106	71.4
	$CsNaX^b$	He	120	102	54.1
	NaY^b	He	144	40	78.3
	$KNaY^b$	He	1158	51	95.8
	$CsNaY^b$	He	1052	51	95.4
(B)	$CaCsNaY^{b,c}$	He	1025	43	96.0
	$CsNaY^b$	He	1052	51	95.4
(C)	$Cs\text{–}Ace/Cs_{39}Na_{19}Y^d$	He	3497	94	97.4
	$Cs\text{–}Ace/Cs_{25}Na_{33}Y^d$	He	2555	79	97.0
	$Cs\text{–}Ace/Cs_{56}Na_{26}X^d$	He	527	328	61.6
(D)	$Cs\text{–}Ace/CsNaY^d$	O_2	4313	118	97.3
	$Cs\text{–}Ace/CsNaY^d$	He	3497	94	97.4

[a] Start-up procedure 1.
[b] Exchanged via hydroxide and unrinsed.
[c] Approximately eight Ca^{2+} per unit cell.
[d] Approximately two cesium acetate molecules per unit cell.
[e] Mole per mole of zeolite unit cells per hour.
[f] Percentage acetone selectivity = acetone yield/(acetone yield + propylene yield) × 100%.

Table 2A lists the intrinsic rates of acetone and propylene formation of the hydroxide-exchanged X and Y zeolites. NaX showed considerable propylene activity. Other than NaX, the propylene formation, on a unit cell basis from the alkali-exchanged X zeolite catalysts, was approximately twice that observed from the Y zeolite catalysts. The origin of propylene in alkali-exchanged zeolites is not fully understood. From infrared studies of pyridine adsorbed on NaX (*27*) and NaY (*28*), Ward concluded that there are no detectable Brønsted or Lewis acid sites after calcining the materials at 500°C. However, Brønsted acid sites were detected by pyridine adsorption on the alkaline earth forms of zeolites X and Y after a 500°C calcination. This is consistent with Mirodatos *et al.* (*29, 30*) who showed from IR studies that water can interact with divalent cations of zeolite Y to form Brønsted acid sites. Jacobs *et al.* (*26*) investigated isopropanol dehydration over alkali-exchanged X and Y zeolites and suggested that the observed activity could be a result of polyvalent cations at the impurity level reacting with water to form active acid sites. To investigate the possibility of divalent cations at the impurity level contributing to the propylene activity listed in Table 1A, ~8 Ca^{+2} per unit cell were exchanged into CsNaY–OH-UR. This material was then calcined at 550°C prior to the initiation of the reactant flow. In Table 2B, it is shown that no effect on propylene activity was found upon the addition of ~8 Ca^{2+} cations per unit cell, thus excluding trace divalent cations as the major source of propylene formation. The results shown in Table 2B could be rationalized by the fact that the 550°C calcination may have caused dehydroxylation with irreversible migration

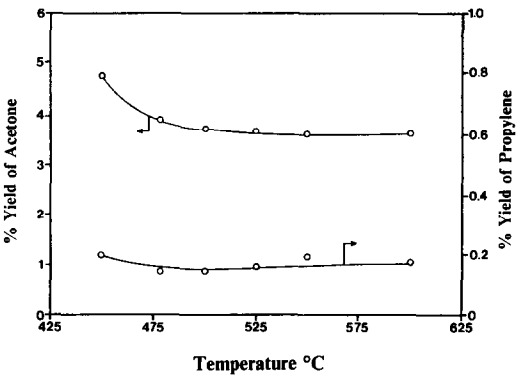

FIG. 2. Effect of the calcination temperature on activity. The calcination atmosphere was helium and the heating rate was 20°C/min. F/W = 1.44 mol isopropanol · h^{-1} · g^{-1}, temperature = 350°C, total pressure = 1 atom, and partial pressure of isopropanol = 152 Torr (STP). Start-up procedure 1.

of the Ca^{2+} cations into the sodalite cages (*26*). Another source for propylene formation on the fully exchanged, unrinsed samples could be from a propoxide intermediate and appears to be a likely candidate at this time (*31*).

Intrinsic rates of acetone formation over the unrinsed hydroxide-exchanged X and Y zeolites are listed also in Table 2A. A large increase in acetone formation was found when Na^{1+} was exchanged by K^{1+} for both zeolites X and Y. For zeolite X, the acetone activity and selectivity were found to be the highest for KNaX. It was the Y zeolite, however, which showed the best acetone activity and selectivity. This enhanced activity of the Y zeolite over the X zeolite was not expected on the basis of data in a prior investigation (*17*) which suggested X zeolite to be more basic. However, the influence of excess alkali must be taken into consideration (*vide infra*).

Because of its high activity and selectivity for acetone formation, zeolite Y exchanged with Cs^{1+} was chosen to investigate further the factors which may influence base activity.

Influence of the calcination temperature. Figure 2 illustrates the yields of acetone and propylene at 350°C as a function of calcination temperature for CsNaY–OH-UR. A small decrease in both the yields of acetone and propylene was observed when the calcination temperature was above 500°C. However, little variation in selectivity was obtained when the catalyst was calcined between 450 and 600°C. The loss in crystallinity from calcination ranged from 4% at 450°C to 11% at 600°C (measured by adsorption).

Interestingly, the rate at which the calcination temperature was achieved played a critical role in the stability of the acetone and propylene activity. Figure 3 shows the effect of the heating rate to reach the calcination temperature on the acetone and propylene activity. These activities were determined using start-up procedure 2 with CsNaY–OH-UR. Two heating rates were employed; 2 and 20°C/min. For both heating rates, the initial acetone and propylene activity were similar. However, for the heating rate of 2°C/min, the acetone activity quickly fell to zero while the propylene activity rose sharply. Attempts to reestablish the initial activity by reactivating the catalyst in helium or air failed. For the heating rate of 20°C/min, both the acetone and the

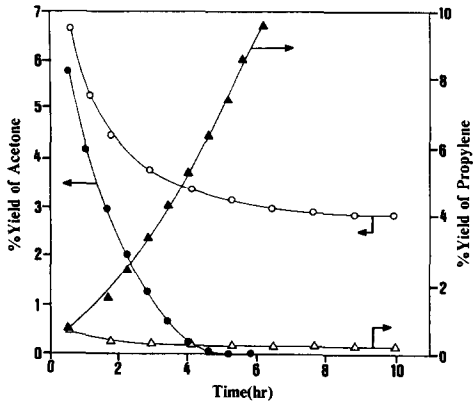

FIG. 3. Effect of the heating rate on activity, 2°C/min: ●, acetone; ▲, propylene; 20°C/min: ○, acetone; △, propylene. F/W = 0.90 mol isopropanol · h^{-1} · g^{-1}, temperature = 350°C, total pressure = 1 atm, and partial pressure of isopropanol = 152 Torr. Start-up procedure 2.

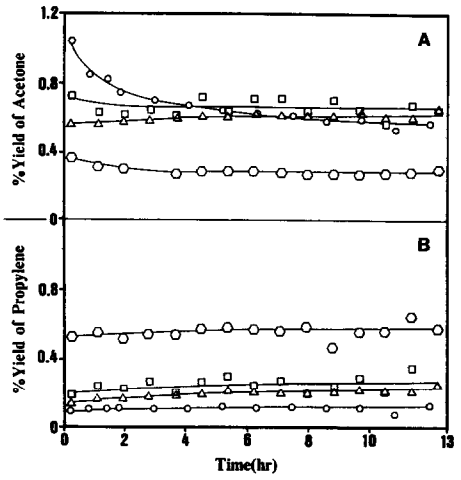

FIG. 4. Effect of the exchange salt on: (A) acetone, and (B) propylene activity of the rinsed zeolite. ○, Hydroxide; □, acetate; △, nitrate; ⬡, chloride. F/W = 2.41 mol isopropanol · h^{-1} · g^{-1}, temperature = 350°C, total pressure = 1 atm, and partial pressure of isopropanol = 152 Torr (STP). Start-up procedure 2.

propylene activity achieved a steady-state value. Little is understood at this point why the heating rate affects the activity, but it does appear from Fig. 3 that the propylene activity is growing at the expense of the acetone activity for the heating rate of 2°C/min.

Influence of the exchange salt. Zeolite Y was exchanged with cesium hydroxide, acetate, nitrate, and chloride to investigate the influence of the exchange salt on activity. Figure 4A shows the effect of the exchange salt on acetone activity of the rinsed catalysts. The hydroxide-, acetate-, and nitrate-exchanged zeolites had approximately the same level of acetone activity with little variation between the initial and the steady-state activity. The cloride-exchanged zeolite showed a lower level of acetone activity which may be a result of occluded chloride (*vide infra*). The propylene activity of the rinsed catalysts is shown in Fig. 4B. Again, approximately the same level of propylene activity was found for the hydroxide-, acetate-, and nitrate-exchanged zeolites. For the chloride-exchanged zeolite, however, a significant increase in propylene activity was observed.

Figure 5 shows the acetone activity of the unrinsed hydroxide-, acetate-, nitrate-, and chloride-exchanged zeolites. For the unrinsed hydroxide- and acetate-exchanged zeolites, the initial acetone activity was increased by a factor of five above the rinsed analogs. This acetone activity slowly declined but remained higher than the activity recorded from the rinsed materials. For the unrinsed nitrate-exchanged zeolite, the acetone activity increased by a factor of two but ultimately reached the activity recorded from its rinsed analog. Interestingly, for the unrinsed, chloride-exchanged zeolite, complete elimination of acetone activity was observed.

The propylene activity (not shown) of the unrinsed hydroxide-, acetate-, and nitrate-exchanged zeolites fell below the activities recorded from the rinsed materials by ~40% suggesting that the higher propylene activity of the rinsed catalysts may be a result of decationation during the rinsing step. Propylene activity for the unrinsed chloride-exchanged zeolite was identical to that of its rinsed analog.

From the results provided thus far, there exist considerable differences in activity

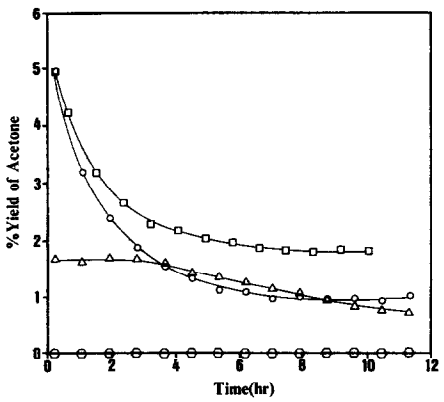

FIG. 5. Effect of the exchange salt on acetone and propylene activity of the unrinsed zeolite. ○, Hydroxide; □, acetate; △, nitrate; ⬡, chloride. F/W = 2.41 mol isopropanol · h^{-1} · g^{-1}, temperature = 350°C, total pressure = 1 atm, and partial pressure of isopropanol = 152 Torr. Start-up procedure 2.

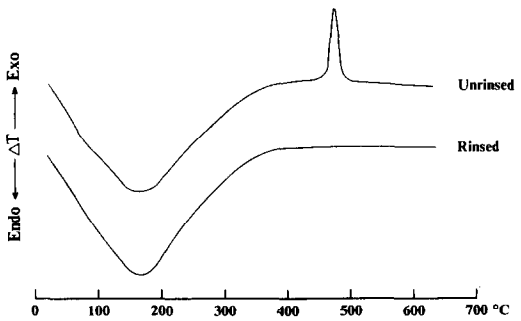

FIG. 6. Differential thermal analysis of the unrinsed and rinsed cesium acetate-exchanged Y zeolite.

between the rinsed and the unrinsed hydroxide- and acetate-exchanged Y zeolites. Two possible explanations could be attributed to these differences. One is that by rinsing the zeolite after filtration, decationation of the zeolite occurs to some degree (thus lowering the acetone activity and increasing the propylene activity). The other possible explanation is that by leaving the zeolite unrinsed, occluded hydroxide or acetate remains which upon calcination provides a second more active base site. To answer these questions, we first establish that by leaving the zeolite unrinsed there is occluded alkali salt. Since the acetate ion (CH_3CHOO^-) is observable by infrared spectroscopy and combustible in air, the unrinsed, acetate-exchanged Y zeolite (CsNaY–Ace-UR) was examined for occluded cesium acetate by infrared spectroscopy and DTA.

Figure 6 shows the DTA patterns for the rinsed and unrinsed acetate-exchanged zeolite. For both cases, the loss of water is reflected by a broad endotherm located between 25 and 350°C. Unlike the rinsed zeolite a sharp exotherm occurs for the unrinsed zeolite at 450°C. Peaks in this region are attributed to the exothermic oxidation of carbon (this peak is absent when the DTA was performed in a helium atmosphere, yet we know the active site is formed in either helium or oxygen (*vide infra*)).

To further investigate the presence of excess cesium acetate, the unrinsed zeolite was examined by FTIR. Figure 7A shows the IR spectrum for cesium acetate pressed in KBr. Kakihana *et al.* (*32*) investigated sodium acetate by infrared spectroscopy. On the basis of their results we have assigned the vibrational frequencies observed for cesium acetate. The broad absorption at 3307 cm^{-1} is in the OH region and is most likely due to trace water. Although not very pronounced, the band observed at 2985 cm^{-1} is assigned to the asymmetric CH_3 stretch. This general weakness, however, is consistent with a CH_3 group adjacent to a carbonyl-derived group such as COO^-(*4*). The band at 1570 cm^{-1} is assigned to the asymmetric CO stretch. For sodium acetate, several frequencies were assigned in the 1440- to 1420-cm^{-1} region. The main contribution, however, occurs from the asymmetric CH_3 deformation and the symmetric CO stretch. Therefore, the band observed at 1399 cm^{-1} in the cesium acetate spectrum is most likely due to one or more of those vibrations. The small shoulder at 1334 cm^{-1} is identical to the value reported by Kakihana *et al.* for the symmetric CH_3 deformation.

For the unrinsed zeolite, a spectrum was recorded at 250, 350, and 450°C in air. The asymmetric and symmetric C–H bands at 2955 and 2911 cm^{-1} are very strong at 250°C clearly indicating the presence of occluded acetate. These bands appear also at 350°C, but disappear after ~30 min (Fig. 7D). At 450°C several bands are still present. The band at 3732 cm^{-1} is assigned to the terminating silanol group and is in good agreement with the value of 3740 cm^{-1} reported by Ward (*33*) for CsNaY. Small broad bands are observed also at 450°C between 1710 and 1366 cm^{-1} which are in the region for carbonate absorption. The band at 2143 cm^{-1} is not assigned as yet.

The absorptions for the acetate ion at 1570 and 1399 cm^{-1} (Fig. 7A) appear to align with the bands at 1578 and 1378 cm^{-1} for the unrinsed zeolite (Fig. 7B). However, we have assigned the band at 1578

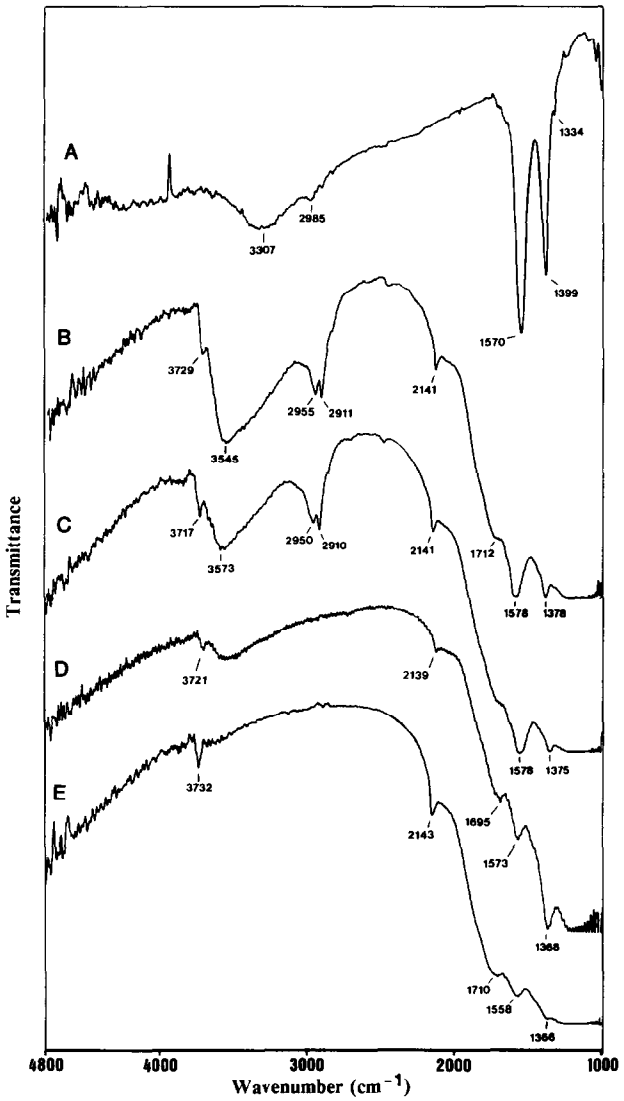

FIG. 7. FTIR spectra of: (A) cesium acetate in KBr at 25°C; the unrinsed cesium acetate-exchanged Y zeolite at (B) 250°C; (C) 350°C for 5 min; (D) 350°C for 30 min; (E) 450°C in air.

cm^{-1} as overlapping CO stretching bands for the occluded acetate ion and also a carbonate species. Furthermore, the band at 1378 cm^{-1} appears to be strictly from a carbonate species. These assignments are supported by the FTIR studies of CsNaY–OH-UR (Figs. 8B and 8C) which contains no acetate ions but has similar base properties to CsNaY–Ace-UR (*vide supra*). Figures 8B and 8C show the IR spectra of CsNaY–OH-UR in air at 150 and 350°C, respectively. The doublet at 1381 and 1317 cm^{-1} (Fig. 8B) along with the band at 1580 cm^{-1} (Fig. 8C) which appear after removal of water (1647 cm^{-1}) are in fair agreement with Bertsch and Habgood (*34*) who observed from CO_2 adsorption on KNaX bands at 1570, 1380, and 1340 cm^{-1}. CsNaY–Ace-UR at 150°C (Fig. 8A) shows a similar doublet at 1387 and 1329 cm^{-1}. However, a

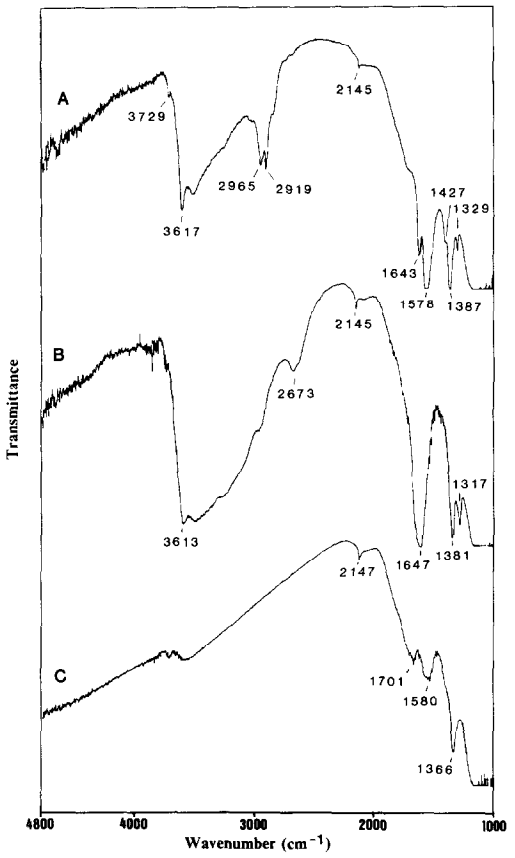

FIG. 8. FTIR spectra of: (A) CsNaY–Ace-UR at 150°C; (B) CsNaY–OH-UR at 150°C; and (C) CsNaY–OH-UR at 350°C in air.

strong absorption at 1578 cm^{-1} along with a shoulder at 1427 cm^{-1} appears also. The band at 1578 cm^{-1} is postulated to be the asymmetric CO stretch of the occluded acetate ion. The shoulder observed at 1427 cm^{-1} which is in the region of 1440–1420 cm^{-1} reported by Kakihana *et al.* for sodium acetate is postulated to be resulting from the occluded acetate as well. Note that after the C–H stretch has disappeared at 350°C (Fig. 7D) (suggesting the decomposition of the acetate) the bands at 1573 and 1368 cm^{-1} are still present. Bands in this region are observed also for the CsNaY–OH-UR at 350°C at 1580 and 1366 cm^{-1} supporting further their assignment to carbonate species.

Carbonate absorptions at 1580 and 1381 cm^{-1} are observed momentarily for the rinsed, acetate-exchanged Y zeolite at 150°C (not shown). However, they disappear upon further heating. The higher thermal stability of the carbonates on the unrinsed, hydroxide- and acetate-exchanged CsNaY zeolites agrees with the results of King and Garces (*35*) who observed that the temperature required to eliminate carbonates from the less basic LiX and NaX zeolites occurred at approximately 400°C. However, they detected considerable amounts of carbonate on the KNaX, RbNaX, and CsNaX at 450°C. King and Garces suggested that this increase in the thermal stability of the carbonates is a result of the higher base strength associated with the K^{1+}, Rb^{1+}, and Cs^{1+}-exchanged X zeolites.

From DTA and FTIR spectroscopy, cesium acetate was detected on the unrinsed zeolite while it was not for the rinsed zeolite. Also, the reaction rate data clearly show a significant increase in acetone activity for the unrinsed, acetate-exchanged zeolite. It, therefore, appears that the differences in activity between the rinsed and the unrinsed, hydroxide- and acetate-exchanged zeolites are not due to a loss in activity from decationation but rather a gain in activity associated with the occluded exchange salt. If this is the case, a second type of base site formed by the decomposition of the occluded cesium salt may be present.

Influence of cesium loading. Cesium was exchanged into NaY at loadings of ~1 Cs^{1+} per unit cell to a full exchange of 39 Cs^{1+} per unit cell (maximum exchange obtained here with a 0.1 *N* solution). The fully exchanged and all partially exchanged zeolites were rinsed with deionized water to remove any residual exchange salt. Cesium loadings above 100% ion exchange were achieved by occluding via exposure to exchange solutions of 0.3–0.5 *N* between 3 and 5 cesium acetate molecules per unit cell into the fully exchanged Y zeolite. Figure 9

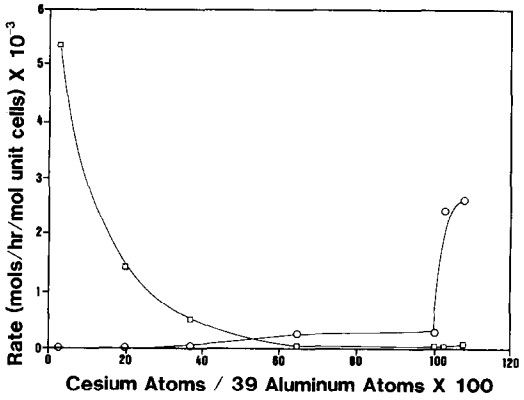

FIG. 9. Effect of cesium loading on activity. ○, Acetone; △, propylene. Temperature = 350°C, total pressure = 1 atm, and partial pressure of isopropanol = 152 Torr (STP). Start-up procedure 1.

illustrates the effect of cesium loading on both acetone and propylene activity. The catalysts with lower levels of cesium showed no detectable acetone formation but very high rates of propylene formation. The high propylene activity was most likely the result of decationation from the rinsing, for very little propylene activity was recorded from the unrinsed NaOH-exchanged Y zeolite (Table 2A). However, as more Cs^{1+} was exchanged into the zeolite the propylene rate declined while the acetone rate rose. Only after 100% ion exchange was exceeded and between 3 and 5 excess cesium acetate molecules per unit cell were occluded into the zeolite does an abrupt rise in the acetone activity occur. It is this abrupt rise that strongly suggests the presence of a second very active base site which appears to be from the decomposition products of the cesium acetate. Acetone activity associated with the rinsed CsNaY could, therefore, be resulting from the lattice oxygens as suggested by other authors (*14, 17*).

Influence of CO_2 contact. Because of the electrophilic nature of CO_2, adsorption onto active base sites, e.g., O^{2-}, can occur and subsequently block base-catalyzed activity (*36*). Furthermore, the nature of the base site can effect the adsorption of CO_2 (*36*) as well as the thermal stability of the adsorbed species. We might, therefore, expect different catalytic behavior during and perhaps after CO_2 contact (*37*). Both the rinsed and the unrinsed Y zeolite exchanged with cesium hydroxide, acetate, nitrate, and chloride were contacted with CO_2 during reaction conditions. After steady state was achieved, CO_2 was introduced into the reactant feed at 5 Torr for 2 h (helium was decreased to maintain a constant partial pressure of isopropanol).

For the rinsed zeolites (Fig. 10), acetone activity was suppressed in the presence of CO_2. Upon removal of CO_2 from the feed which contacted the acetate-, nitrate-, and chloride-exchanged zeolites, the acetone activity returned immediately to the steady-state value. Upon CO_2 removal from the feed which contacted the rinsed hydroxide-exchanged zeolite, a small increase in acetone activity was observed which may suggest incomplete rinsing of the zeolite (*vide infra*).

Figure 11 shows the influence of CO_2 on the acetone activity of the unrinsed zeolites. The acetone activity of the unrinsed hydroxide- and acetate-exchanged zeolites was very high initially, but declined slowly to lower levels of activity. Contact of CO_2 with these catalyst suppressed acetone activity. Upon removal of CO_2 from the feed, the high activity observed at initial times was reestablished which may suggest that some base sites were being reactivated by CO_2 contact. Further evidence to suggest that some base sites could be reactivated by CO_2 contact and removal is given by the activity data from the unrinsed, nitrate-exchanged zeolite. As shown in Fig. 11, the initial and steady-state acetone activity of the unrinsed nitrate-exchanged zeolite are fairly similar. However, after CO_2 contact, the acetone activity was promoted to the high levels observed for the unrinsed hydroxide- and acetate-exchange zeolites.

Effect of support. To investigate the role

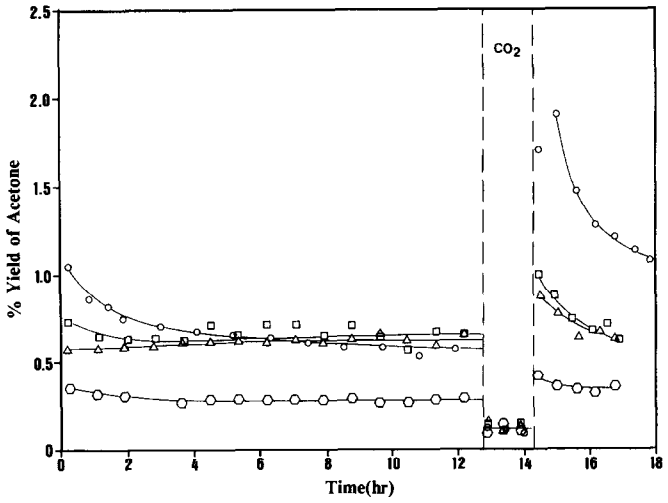

FIG. 10. Effect of CO_2 contact on the activity of rinsed Y zeolites. ○, Hydroxide; □, acetate; △, nitrate; ⬡, chloride. F/W = 2.41 mol isopropanol · h^{-1} · g^{-1}, temperature = 350°C, total pressure = 1 atm, and partial pressure of isopropanol = 152 Torr (STP). Start-up procedure 2.

of the CsNaY zeolite in the formation of the base site via cesium acetate decomposition, cesium acetate was impregnated at ~2.4 wt% on CsNaY, silica gel, and activated carbon. Figures 12B and 12D show the DTA patterns for the decomposition of cesium acetate on CsNaY and the silica gel, respectively. For the silica support, a broad exotherm is shown at 300°C. However, for CsNaY a sharp exotherm occurs at ~475°C suggesting the decomposition mechanism differs for the two supports. Also, cesium acetate supported on silica gel and activated carbon showed no acetone formation at 350°C, and only trace propylene activity was observed for the silica support. From

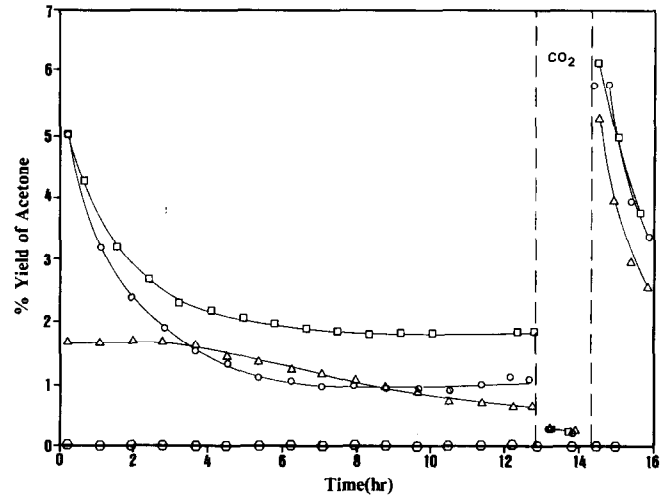

FIG. 11. Effect of CO_2 contact on the activity of unrinsed Y zeolites. ○, Hydroxide; □, acetate; △, nitrate; ⬡, chloride. F/W = 2.41 mol isopropanol · h^{-1} · g^{-1}, temperature = 350°C, total pressure = 1 atm, and partial pressure of isopropanol = 152 Torr (STP). Start-up procedure 2.

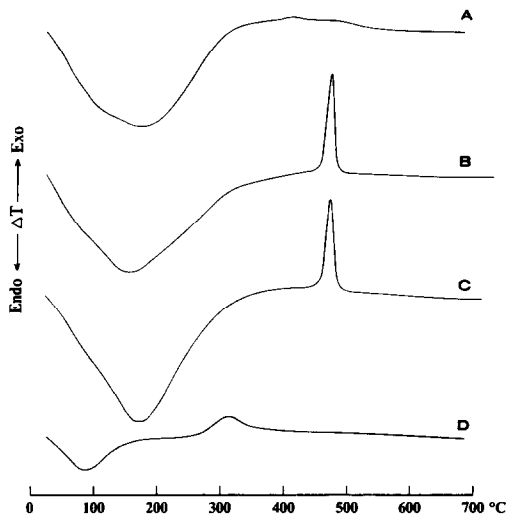

FIG. 12. Differential thermal analysis of: (A) 2.0 Cs–Ace/$Cs_{56}Na_{26}X$; (B) 2.0 Cs–Ace/$Cs_{39}Na_{19}Y$; (C) 2.0 Cs–Ace/$Cs_{25}Na_{33}Y$; (D) 2.4 wt% Cs–Ace/SiO_2.

the reaction rate data and DTA patterns, it appears that CsNaY does play an active role in the decomposition of the cesium acetate to an active base site.

It was shown previously that CsNaX–OH-UR was less effective for acetone formation than CsNaY–OH-UR (Table 2A). To investigate this further, cesium acetate was impregnated at approximately 2.0 cesium acetate molecules per unit cell into (i) a $Cs_{56}Na_{26}X$ zeolite, (ii) a fully exchanged $Cs_{39}Na_{19}Y$ zeolite, and (iii) a partially exchanged $Cs_{25}Na_{33}Y$ zeolite. Infrared studies confirm the presence of occluded cesium acetate for these three catalysts. Because zeolite X is difficult to fully exchange, the partially exchanged Y zeolite (iii) was also used to investigate the possibility that during the impregnation of the X zeolite, Na^{1+} ions were being exchanged by the cesium acetate to form sodium acetate. Table 2C gives the rate of acetone and propylene formation per unit cell for the three catalysts. The partially exchanged Y zeolite showed high acetone activity and selectivity. Therefore, we exclude the possibility that all the cesium acetate exchanges with Na^{+1} ions during impregnation. Again, low acetone activity and selectivity were found for the X zeolite. To determine whether the decomposition mechanism of the acetate is similar for the X and Y zeolite, differential thermal analysis was performed in air. From Fig. 12, the fully and partially exchanged Y zeolites have the sharp exotherm at 475°C suggesting that the decomposition of the acetate occurs in an identical fashion on these materials. However, this decomposition process does not appear to occur for the X zeolite as evidenced by the small broad exotherm located between 350 and 500°C.

Influence of the calcination atmosphere. CsNaY impregnated with ~2.4 wt% cesium acetate was calcined with helium (99.995$^+$%) and oxygen (99.5$^+$%) to investigate how these gases influence the decomposition of the acetate to an active base site. The results are given in Table 2D. With the oxygen calcination, both the acetone and the propylene activity were slightly greater than that obtained from the helium atmosphere. Interestingly, the calcination atmosphere had no effect on selectivity. This might suggest that the decomposition mechanism is similar in both calcination atmospheres; however, the oxygen calcination appears to be slightly more effective for the production of active sites.

Comparison to MgO. MgO formed by the dehydroxylation of $Mg(OH)_2$ was used here so that a comparison could be made between our zeolite activities here and those reported in the open literature for other metal oxides. From data given by Tanabe (*38*), it was shown that to achieve the optimal number of base sites in the transformation of $Mg(OH)_2$ to MgO, the calcination temperature should be between 550 and 600°C. Therefore, $Mg(OH)_2$ was heated in helium to 550°C for 4 h. Start-up procedure 1 was used to determine the reaction rates. Table 3 shows that on a surface area basis, the acetone activity for CsNaY zeolite modified with ~2.4 wt% cesium acetate is slightly greater than that observed for the MgO catalyst at 350°C.

TABLE 3

Activity of MgO[a] and CsNaY[b]

Catalyst	BET area (m^2/g)[c]	Acetone rate ($mol/h/m^2 \times 10^6$)	Propylene rate ($mol/h/m^2 \times 10^6$)	% Acetone selectivity[d]
MgO[a]	125	334	7.9	97.7
Cs–Ace/CsNaY[b]	492	406	10.9	97.4

[a] Derived from $Mg(OH)_2$.

[b] Approximately two cesium acetate molecules per unit cell.

[c] BET surface areas calculated from O_2 adsorption data.

[d] Percentage acetone selectivity = acetone yield/(acetone yield + propylene yield) × 100%.

CONCLUSIONS

It is concluded from this work that upon calcination, a very active base site is formed by the decomposition of cesium acetate supported on CsNaY zeolite. Upon impregnation of CsNaX and CsNaY with identical loadings of cesium acetate, the acetone activity of the impregnated CsNaY zeolite is an order of magnitude greater than that found for the impregnated CsNaX zeolite. The impregnated CsNaY is found also to show an order of magnitude greater acetone activity than the parent CsNaY zeolite. Furthermore, for the impregnated CsNaY zeolite, the selectivity to acetone is above 97%, and on a surface area basis, the acetone activity is slightly greater than MgO at 350°C.

ACKNOWLEDGMENTS

Financial support of this work is provided by the National Science Foundation and the Dow Chemical Co. under the Presidential Young Investigator Award to M.E.D.

REFERENCES

1. Barthomeuf, D., Coudurier, G., and Vedrine, J. C., *Mater. Chem. Phys.* **18,** 553 (1988).
2. Krylov, O. V., "Catalysis by Non-Metals," p. 118. Academic Press, New York, 1970.
3. Gentry, S. J., and Rudham, R., *J. Chem. Soc. Faraday Trans. 1* **70,** 1685 (1974).
4. Zaki, M. I., and Sheppard, N., *J. Catal.* **80,** 114 (1983), and references therein.
5. Miyata, H., Wakamiya, M., and Kubokawa, Y., *J. Catal.* **34,** 117 (1974).
6. Koga, O., Onishi, T., and Tamaru, K., *J. Chem. Soc. Faraday Trans. 1* **76,** 19 (1980).
7. Kim, K. S., Barteau, M. A., and Farneth, W. E., *Langmuir* **4,** 533 (1988).
8. Parrott, S. L., Rodgers, J. W., Jr., and White, J. M., *Appl. Surf. Sci.* **1,** 443 (1978).
9. Bowker, M., Petts, R. W., and Waugh, K. C., *J. Chem. Soc. Faraday Trans. 1* **81,** 3073 (1985).
10. Waugh, K. C., Bowker, M., Petts, R. W., Vandervell, H. D., and O'Malley, J., *Appl. Catal.* **25,** 121 (1986).
11. Bowker, M., Petts, R. W., and Waugh, K. C., *J. Catal.* **99,** 53 (1986).
12. Noller, H., and Ritter, G., *J. Chem. Soc. Faraday Trans. 1* **80,** 275 (1984).
13. Cunningham, J., Hodnett, B. K., Ilyas, M., Tobin, J., and Leahy, E. L., *Discuss. Faraday Soc.* **72,** 283 (1981).
14. Yashima, T., Suzuki, H., and Hara, N., *J. Catal.* **33,** 486 (1974).
15. Nagy, J. B., Lange, J.-P., Gourge, A., Bodart, P., and Gabelica, Z., *in* "Catalysis by Acids and Bases" (B. Imelik *et al.*, Eds.), Vol. 20, p. 127. Elsevier, Amsterdam, 1980.
16. Derewinski, M., Haber, J., and Ptaszynski, J., *in* "New Developments in Zeolite Science and Technology: Proceedings of the 7th International Zeolite Conference, Tokyo, Japan, August 17–22, 1986" (Y. Murakami *et al.*, Eds.), p. 57. Elsevier, Amsterdam, 1986.
17. Barthomeuf, D., *J. Phys. Chem.* **88,** 42 (1984).
18. Unland, M. L., and Baker, G. E., *in* "Catalysis of Organic Reactions" (W. R. Moser, Ed.), p. 51. Dekker, New York, 1981.
19. Garces, J. M., Vrieland, G. E., Bates, S. I., and Scheidt, F. M., *in* "Catalysis by Acids and Bases" (B. Imelik *et al.*, Eds.), Vol. 20, p. 67. Elsevier, Amsterdam, 1985.
20. Engelhardt, J., Szanyi, J., and Valyon, J., *J. Catal.* **107,** 296 (1987).

21. Martens, L. R., Vermeiren, W. J., Huybrechts, D. R., Grobet, P. J., and Jacobs, P. A., *in* "Proceedings, 9th International Congress on Catalysis, Calgary, 1988" (M. J. Phillips and M. Ternan, Eds.), Vol 1, p. 420. The Chemical Institute of Canada, Ottawa, 1988.
22. Galich, P. N., Golubchenko, I. T., Gutyrya, V. S., Ilín, V. G., and Neimark, I. E., *Ukr. Khim. Zh.* **31**(11), 1117 (1965).
23. Hicks, R. F., Kelher, C. S., Savatsky, B. J., Hecker, W. C., and Bell, A. T., *J. Catal.* **71,** 216 (1981).
24. Dietz, W. A., *J. Gas Chromatogr.* **5,** 67 (1967).
25. Breck, D. W., "Zeolite Molecular Sieves," p. 611. Wiley, New York, 1984.
26. Jacobs, P. A., Tielen, M., and Uytterhoeven, J. B., *J. Catal.* **50,** 98 (1977).
27. Ward, J. W., *J. Catal.* **14,** 365 (1969).
28. Ward, J. W., *J. Catal.* **10,** 34 (1968).
29. Mirodatos, C., Pichat, P., and Barthomeuf, D., *J. Phys. Chem.* **80**(12), 1335 (1976).
30. Mirodatos, C., Kais, A. A., Vedrine, J. C., Pichat, P., and Barthomeuf, D., *J. Phys. Chem.* **80**(21), 2366 (1976).
31. Hathaway, P. E., and Davis, M. E., *J. Catal.* **116,** in press.
32. Kakihana, M., Kotaka, M., and Okamoto, M., *J. Phys. Chem.* **87,** 2526 (1983).
33. Ward, J. W., *J. Phys. Chem.* **72**(12), 4211 (1968).
34. Bertsch, L., and Habgood, H. W., *J. Phys. Chem.* **67,** 1621 (1965).
35. King, S. T., and Garces, J. M., *J. Catal.* **104,** 59 (1987).
36. Peri, J. B., *J. Phys. Chem.* **79**(15), 1582 (1975).
37. Cunningham, J., and Hodnett, B. K., *J. Chem. Soc. Faraday Trans. 1* **77,** 2777 (1981).
38. Tanabe, K., "Solid Acids and Bases," p. 50. Academic Press, New York, 1970.